saturation. The evaluation of this waveguide for such applications would in turn require determination of the equivalent circuit of the ridge–gap mounting structure. That would be the topic of a future communication.

ACKNOWLEDGMENT

The authors are indebted to Prof. B. R. Nag for his helpful suggestions and critical appraisal of the manuscript. Thanks are also due to the Computer Centre, University of Calcutta, for providing the computing facilities.

REFERENCES

[1] S. B. Cohn, "Properties of Ridge Wave Guide," *Proc. IRE*, vol. 35, pp. 783–788, Aug. 1947.
[2] S. Hopfer, "The design of Ridged Waveguides," *IRE Trans. Microwave Theory Tech.*, vol. MTT-3, pp. 20–29, Oct. 1955.
[3] W. J. Getsinger, "Ridge Waveguide Field Description and Applications to Directional Couplers", *IRE Trans. Microwave Theory Tech.*, vol. MTT-10, pp. 41–50, Jan. 1962.
[4] E. V. Jull, W. J. Bleackley, and M. M. Steen, "The Design of Waveguides with Symmetrically Placed Double Ridges," *IEEE Trans. Microwave Theory Tech.*, vol. MTT-17, pp. 397–399, July 1969.
[5] S. Mizushina and T. Ohsuka, "The Ridged-Waveguide-Cavity Gunn Oscillator for Wide-Band Tuning," *IEEE Trans. Microwave Theory Tech.*, vol. MTT-24, pp. 257–259, May 1976.
[6] S. Mizushina, N. Kuwabara, and H. Kondoh, "Theoretical Analysis of a Ridged-Waveguide Mounting Structure," *IEEE Trans. Microwave Theory Tech.*, vol. MTT-25, pp. 1131–1134, Dec. 1977.
[7] J. P. Montgomery, "On the Complete Eigenvalue Solution of Ridged Waveguide," *IEEE Trans. Microwave Theory Tech.*, vol. MTT-19, pp. 547–555, June 1971.

Asymmetric Realizations for Dual-Mode Bandpass Filters

RICHARD J. CAMERON AND JOHN DAVID RHODES, SENIOR MEMBER, IEEE

Abstract—**Two analytic synthesis techniques are presented for even-degree asymmetric dual-mode in-line prototype networks up to degree 14. Commencing with the coupling matrix for the double cross-coupled array, rotational transformations are applied to transform the matrix into the form required for the dual-mode in-line asymmetric structure. "Asymmetric" here means that the coupling elements (irises, screws) are unequal in value about the physical center of the filter. The necessity for these asymmetric solutions arose when it was discovered that it was impossible to realize certain useful transmission characteristics with the symmetric in-line structure, on account of their transmission zero pattern in the complex-plane representation of the transfer function. Furthermore, because the full coupling matrix is used instead of the even-mode matrix as with the symmetric solution, the asymmetric in-line realization process may be applied to electrically asymmetric matrices, such as those for single-ended filters for multiplexer applications. To demonstrate the validity of the theory, a practical model of each type of realization has been constructed and measured.**

I. INTRODUCTION

THE PROBLEM of converting the mathematical describing polynomials of the characteristics of a low-pass prototype filter network into a symmetric in-line dual-mode structure was first addressed by Atia and Williams [1]. Firstly an even-mode coupling matrix was synthesized, and then by iteratively rotating this matrix certain prescribed couplings were annihilated. The resulting matrix, when unfolded into the full coupling matrix, contains only those couplings that could be realized by a symmetric in-line dual mode structure, while retaining the original 2-port electrical parameters. More recently, the procedure of annihilating the couplings by iteration and optimization has been replaced by analytic techniques for even filter orders 6–12 inclusive [2]. These analytic techniques use as their base, the folded coupling matrix for the generalized low-pass cross-coupled network, the synthesis of which is described in [3]. Using these new procedures, the full coupling matrices for symmetric in-line dual-mode filters are easily and quickly generated from the describing polynomials.

The symmetric realizations however have restrictions. Firstly, the methods cannot be used for electrically asymmetric characteristics, such as those for multiplexer applications. Secondly, there does not appear to be a solution for 14th order characteristics, which occasionally do have application. Thirdly, for lower degree cases, certain characteristics which have particular patterns of transmission zeros as represented in the Argand diagram are unrealizable with a symmetric structure. A complete set of realizability conditions is given in [2].

It was these reasons that prompted a study to be made into solutions other than with symmetric structures. In fact two general types of asymmetric solution were discovered. The first is a general asymmetric solution which

Manuscript received May 19, 1980; revised August 28, 1980.
R. J. Cameron is with the European Space Research and Technology Centre, 2200 AG, Noordwijk, The Netherlands.
J. D. Rhodes is with the Department of Electrical and Electronic Engineering, The University, Leeds LS2 OJT, England.

0018-9480/81/0100-0051$00.75 ©1981 IEEE

is valid for realization of any network transfer function, including those characteristics which lie in the areas mentioned above and which cannot be realized with the symmetric structure. The second type is known as the cascade-quadruplet (CQ) in-line solution, which has different restrictions to the symmetric solution. The general realizability condition in this case is that the transfer function cannot have complex transmission zeros. For both types of realization, a description of the analytic methods leading to the in-line realization is presented, for even orders 6–14 inclusive for the general solution, and for even orders 6–10 inclusive for the CQ solution. A laboratory model of each type has been constructed and the measured performance of each is given.

II. General Principles

As with the symmetric solution, both the solutions described here use as their base the generalized low-pass cross-coupled network (Fig. 1(a)). The synthesis procedure for this network is given in [3]. The network is a folded ladder network of admittance inverters K_i and shunt capacitors C_i, cross coupled by further inverters K_j'. Fig. 1(b) shows the corresponding coupling and routing diagram for this network, where the capacitors are depicted as nodes intercoupled by forward and cross couplings M_{ij}. Fig. 1(c) gives the coupling matrix for the generalized cross-coupled network together with the formulas used to generate the elements of the matrix from the elements of the network. The procedure is equivalent to scaling the internal capacitors of the network to the normalized value of unity.

Relating the diagram of Fig. 1(b) to the coupling matrix of Fig. 1(c) it is clear that the main couplings are those running parallel to the principle diagonal, i.e., M_{12}, M_{23}, M_{34}, etc. The weaker cross couplings are those on the antidiagonal, M_{18}, M_{27}, M_{36} in this case. There are three cross couplings in this example, but when converting this folded configuration coupling matrix to that for an in-line configuration, one must be mindful of the fact that the folded configuration realizes the maximum number of couplings for a given order, and therefore the maximum number of finite location transmission zeros. The in-line configuration is able to realize less finite zeros, according to the rule

$$\left.\begin{array}{l}\text{maximum number of}\\ \text{realizable finite}\\ \text{zeros with in-line}\\ \text{realization}\end{array}\right\}\begin{array}{ll} m=N/2 & (n \text{ even})\\ m=(N/2-1) & (n \text{ odd})\end{array} \quad (1)$$

where $n=N/2$ and N is the order of the filter. Before committing a transfer function to the in-line realization process it should always be tested to ensure that the number of finite zeros required to realize it does not exceed m. A $N\times N$ rotation matrix $\boldsymbol{R}$ is defined as in Fig. 2. Pivot $[i, j]$ means that $R_{ii}=R_{jj}=\cos\theta_r$, and $R_{ji}=-R_{ij}=\sin\theta_r$ $(i, j\neq 1 \text{ or } N)$. If a coupling matrix $\boldsymbol{M}$ is premultiplied by $\boldsymbol{R}$ and the result postmultiplied by $\boldsymbol{R}^{\mathrm{T}}$ (the transpose of $\boldsymbol{R}$) a new matrix will result which has the same eigenvalues and eigenvectors as the original $\boldsymbol{M}$

$$\boldsymbol{M}_r=\boldsymbol{R}_r\cdot\boldsymbol{M}_{r-1}\cdot\boldsymbol{R}_r^{\mathrm{T}} \qquad (r=1,2,3,\cdots). \quad (2)$$

An infinite number of networks therefore exist which, if all the couplings within the resultant coupling matrix are realized, will produce the same transfer function as the original.

The essence of the general in-line realization method to be described below is to apply a series of rotations according to (2), where the angle of rotation θ_r of the rth rotation is derived from elements of the coupling matrix resultant from the $(r-1)$th rotation. The first rotation is applied to the generalized cross-coupled array matrix $\boldsymbol{M}_0$ (Fig. 1(c) and after the final rotation the goal is to achieve the

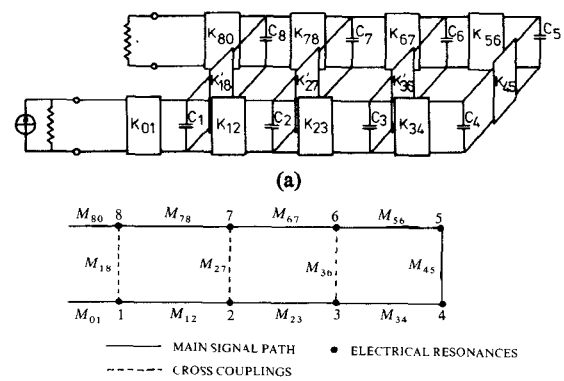

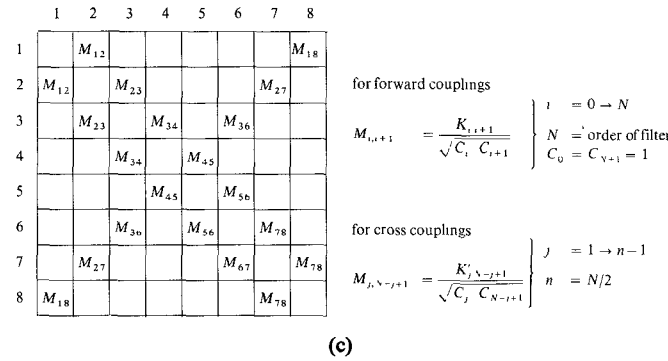

Fig. 1. (a) Generalized low-pass cross-coupled network. (b) Coupling and routing schematic (8th order example). (c) Coupling matrix for low-pass prototype (8th order example).

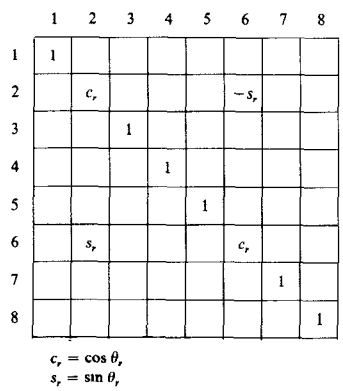

Fig. 2. 8×8 rotation matrix example, pivot (2,6), angle θ_r.

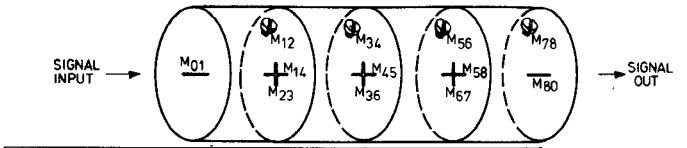

PHYSICAL CAVITY NO		1	2	3	4
CONTAINING ELECTRICAL RESONANCE NUMBERS	VERTICAL POLARISATION	2	3	6	7
	HORIZONTAL POLARISATION	1	4	5	8

(a)

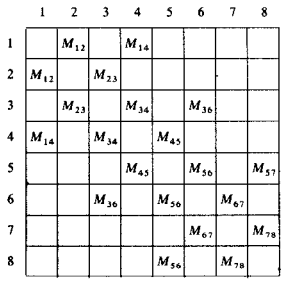

(b)

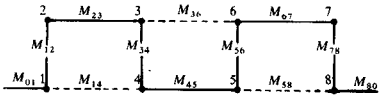

(c)

Fig. 3. (a) In-line dual-mode structure, 8th order example. (b) In-line structure coupling matrix. (c) Coupling and signal routing schematic.

coupling matrix which may be realized by an asymmetric in-line dual mode structure (Fig. 3).

III. General Asymmetric Solution

Unfortunately there does not seem to be any pattern governing the pivotal positions or angle of rotation for different orders of filter. Each (even) order has to be considered individually. For $N=4$ the cross coupled array matrix and dual mode in line prototype are of the same structural form and further transformation is not necessary. $N=6$ is the first nontrivial case, and solutions for $N=6$, 8, 10, 12, and 14 have been derived. Table I gives a summary of the pivotal positions and angles θ_r of the series of rotations that have to be applied in order according to (2). It should be noted that when calculating the angle of rotation θ_r for the rth rotation, the elements $M_{u1,u2}$ and $M_{v1,v2}$ are taken from the coupling matrix resultant from the previous rotation, and that the rotation is then applied to this resultant matrix.

There are no conditions on the pattern of the zeros of the transfer functions for an in-line solution using this method, provided the total number of finite-location zeros $z \leqslant m$ as previously described.

If the rotations of Table I are successively applied to the cross-coupled array matrix, a coupling matrix will emerge that is realizable in an in-line dual mode structure with asymmetric-valued coupling elements. A point of interest here is that for n odd, one of the internal irises next to the input or output coupling iris will be a slot, unlike the rest which will be cruciform. A 14th order linear phase filter has been designed and constructed using these techniques, and a description and measured

TABLE I
Pivotal Positions and Rotation Angles for General Asymmetric In-Line Realizations, Orders 6 (2) 14

Order N	Rotation Number r	Pivot $[i,j]$	$\theta_r=\tan^{-1}(k\ M_{u1,u2}/M_{v1,v2})$ $u1$	$u2$	$v1$	$v2$	k
6	1	[2, 4]	2	5	4	5	+1
8	1	[4, 6]	3	6	3	4	−1
	2	[2, 4]	2	7	4	7	+1
	3	[3, 5]	2	5	2	3	−1
	4	[5, 7]	4	7	4	5	−1
10	1	[4, 6]	4	7	6	7	+1
	2	[6, 8]	3	8	3	6	−1
	3	[7, 9]	6	9	6	7	−1
12	1	[5, 9]	4	9	4	5	−1
	2	[3, 5]	3	10	5	10	+1
	3	[2, 4]	2	5	4	5	+1
	4	[6, 8]	3	8	3	6	−1
	5	[7, 9]	6	9	6	7	−1
	6	[8, 10]	5	10	5	8	−1
	7	[9, 11]	8	11	8	9	−1
14	1	[6, 10]	5	10	5	6	−1
	2	[4, 6]	4	11	6	11	+1
	3	[7, 9]	4	9	4	7	−1
	4	[8, 10]	7	10	7	8	−1
	5	[9, 11]	6	11	6	9	−1
	6	[10, 12]	9	12	9	10	−1
	7	[5, 7]	4	7	4	5	−1
	8	[7, 9]	6	9	6	7	−1
	9	[9, 11]	8	11	8	9	−1
	10	[11, 13]	10	13	10	11	−1

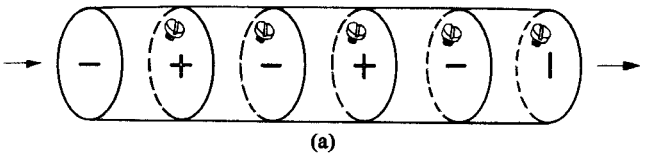

(a)

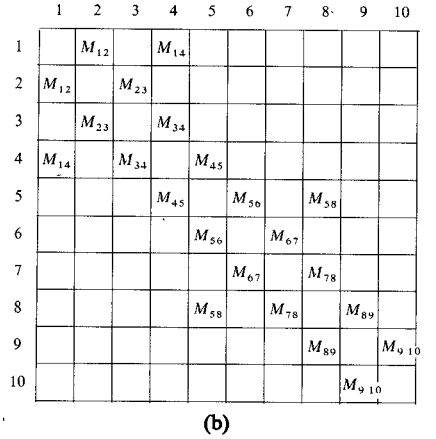

(b)

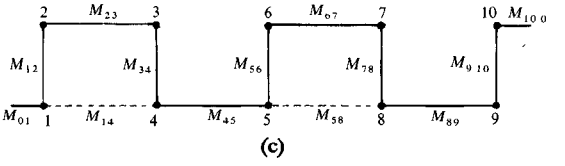

(c)

Fig. 4. (a) 10th order example of a CQ dual-mode structure. (b) Coupling matrix for 10th order CQ example. (c) Coupling and routing diagram.

curves of its performance will be found towards the end of this paper.

IV. Cascade Quadruplet Realization

A CQ construction is similar to the general asymmetric structure described above, but the internal irises are alternately cruciform and slot along the length of the filter (Fig. 4(a)). From the coupling and routing diagram of Fig.

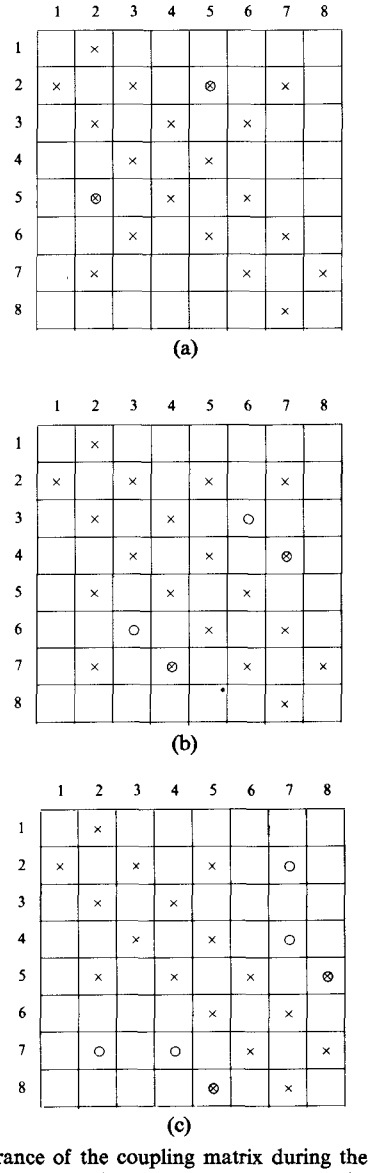

Fig. 5. Appearance of the coupling matrix during the first three rotations. × Nonzero coupling matrix entry. ⊗ Coupling matrix entries that have been created as a consequence of a rotation. ○ Coupling matrix entries that have been annihilated as a consequence of a rotation.

TABLE II
ROTATIONS FOR THE 8TH ORDER CQ SOLUTION

Rotation number r	Pivot $[i,j]$	$\theta_r = \tan^{-1}(k\ M_{u1,u2}/M_{v1,v2})$ $u1$	$u2$	$v1$	$v2$	k
1	[3, 5]					+1
2	[4, 6]	3	6	3	4	−1
3	[5, 7]	4	7	4	5	−1
4	[2, 4]	2	5	4	5	+1

4(c) it may be seen that the nodes are arranged in quadruplets, each with one cross coupling, and connected in cascade with each other through one main-line coupling. For n odd an extra pair of nodes is attached at the end. Each quartet may be identified with the production of a transmission zero pair. If the cross coupling is negative an imaginary axis pair will be created, there producing an attenuation pole pair, and if it is positive a real-axis pole pair will result with group delay self-equalization.

The value of this CQ structure is not so much that it saves on coupling irises, but that it is able to realize those characteristics that violate the conditions of realization for the symmetric structure, on account of their transmission zero pattern. It has provided an elegant solution to the very useful 8th order characteristic which has one real axis and one imaginary axis transmission zero pair, which violates the conditions of realizability for the symmetric structure.

The base is again the coupling matrix for the generalized cross-coupled network, Fig. 1(c). The solution for the 6th order case is the same as that for the general in-line solution. That this is so becomes clear when the coupling and routing diagram is drawn for the 6th order case and remembering that for n odd the general in-line solution produces one zero-value internal cross coupling. The first order that will be considered for the CQ solution will therefore be the 8th.

A. 8th Order CQ Solution

Rotations are applied to coupling matrices in exactly the same manner as described for the general asymmetric solution. The difference here is that the first rotation is by an unknown angle θ_1. Two further rotations are then made in accordance with Table II.

Fig. 5 shows the nonzero entries in the coupling matrix after each of the first three rotations. Each entry is indicated with a cross for convenience, but the actual value of each element will probably change after each rotation. Adopting the notations $t_1 \equiv \tan\theta_1$, $c_3 \equiv \cos\theta_3$, etc., and $M'_{ij} \equiv$ matrix element after first rotation, M'''_{ij} after third rotation, etc., the following equation sets appear (matrix elements after a rotation expressed in terms of those before the rotation):

1) After First Rotation:

$$\begin{aligned} M'_{12} &= M_{12} \\ M'_{23} &= c_1 M_{23} \\ M'_{34} &= c_1 M_{34} - s_1 M_{45} \\ M'_{45} &= s_1 M_{34} + c_1 M_{45} \\ M'_{56} &= s_1 M_{36} + c_1 M_{56} \\ M'_{67} &= M_{67} \\ M'_{78} &= M_{78} \\ M'_{36} &= c_1 M_{36} - s_1 M_{56} \\ M'_{25} &= s_1 M_{23} \\ M'_{27} &= M_{27}. \end{aligned} \tag{3}$$

2) After Second Rotation:

$$\begin{aligned} M''_{12} &= M'_{12} \\ M''_{23} &= M'_{23} \\ M''_{34} &= c_2 M'_{34} - s_2 M'_{36} \\ M''_{45} &= c_2 M'_{45} - s_2 M'_{56} \\ M''_{56} &= s_2 M'_{45} + c_2 M'_{56} \\ M''_{67} &= c_2 M'_{67} \\ M''_{78} &= M'_{78} \\ M''_{25} &= M'_{25} \\ M''_{27} &= M'_{27} \\ M''_{47} &= -s_2 M'_{67} \\ M''_{36} &= s_2 M'_{34} + c_2 M'_{36} = 0 \text{ because } t_2 = -M'_{36}/M'_{34}. \end{aligned} \tag{4}$$

3) After Third Rotation:

$$\begin{aligned}
M_{12}''' &= M_{12}'' \\
M_{23}''' &= M_{23}'' \\
M_{34}''' &= M_{34}'' \\
M_{45}''' &= c_3 M_{45}'' - s_3 M_{47}'' \\
M_{56}''' &= c_3 M_{56}'' - s_3 M_{67}'' \\
M_{67}''' &= s_3 M_{56}'' + c_3 M_{67}'' \\
M_{78}''' &= c_3 M_{78}'' \\
M_{58}''' &= -s_3 M_{78}'' \\
M_{25}''' &= c_3 M_{25}'' - s_3 M_{27}'' \\
M_{27}''' &= s_3 M_{25}'' + c_3 M_{27}'' \\
M_{47}''' &= s_3 M_{45}'' + c_3 M_{47}''.
\end{aligned} \tag{5}$$

To force M_{27}''' and M_{47}''' in (5) simultaneously to zero, t_3 is set equal to $-M_{27}''/M_{25}''$. Then

$$M_{25}'' M_{47}'' = M_{45}'' M_{27}''$$

and substituting from (4)

$$\frac{M_{25}'}{c_2 M_{45}' - s_2 M_{56}'} = \frac{M_{27}'}{-s_2 M_{67}'}$$

or

$$\frac{M_{25}'}{M_{34}' M_{45}' + M_{36}' M_{56}'} = \frac{M_{27}'}{M_{36}' M_{67}'}. \tag{6}$$

Substituting for M_{ij}' in (6) using (3) yields, after a good deal of algebraic manipulation, a quadratic equation for t_1 in terms of the elements of M_0, the original cross-coupled network matrix.

One further rotation is necessary, defined in Table II, in order to annihilate M_{25}'' (Fig. 5(c)), after which the CQ matrix of Fig. 6(a) appears. Fig. 6(b) gives the routing and coupling diagram for the 8th order CQ structure, and the explicit formulas (7) give the four rotation angles and the elements of the final CQ coupling matrix, all in terms of the coupling elements of the original cross-coupled network matrix M_0

$$M_{12}^{IV} = c_4 M_{12} \qquad M_{23}^{IV} = c_1 c_4 \left[M_{23} - \frac{t_4}{c_2} (M_{34} - t_1 M_{45}) \right]$$

$$M_{78}^{IV} = c_3 M_{78} \qquad M_{34}^{IV} = c_1 c_4 \left[t_4 M_{23} + \frac{1}{c_2} (M_{34} - t_1 M_{45}) \right]$$

$$M_{14}^{IV} = s_4 M_{12} \qquad M_{45}^{IV} = \frac{-M_{27}}{s_3 s_4}$$

$$M_{58}^{IV} = -s_3 M_{78} \qquad M_{56}^{IV} = c_2 c_3 \left[\frac{1}{c_1} (M_{56} + t_2 M_{45}) - t_3 M_{67} \right]$$

$$M_{67}^{IV} = c_2 c_3 \left[\frac{t_3}{c_1} (M_{56} + t_2 M_{45}) + M_{67} \right] \tag{7}$$

where t_1 is the solution of the quadratic equation

$$\begin{aligned}
&t_1^2 (M_{27} M_{45} M_{34} - M_{36} M_{67} M_{23} + M_{36} M_{56} M_{27}) \\
&\quad + t_1 \left(M_{23} M_{67} M_{36} - M_{27} \left(M_{36}^2 - M_{56}^2 - M_{45}^2 + M_{34}^2 \right) \right) \\
&\quad - M_{27} (M_{56} M_{36} + M_{34} M_{45}) = 0
\end{aligned}$$

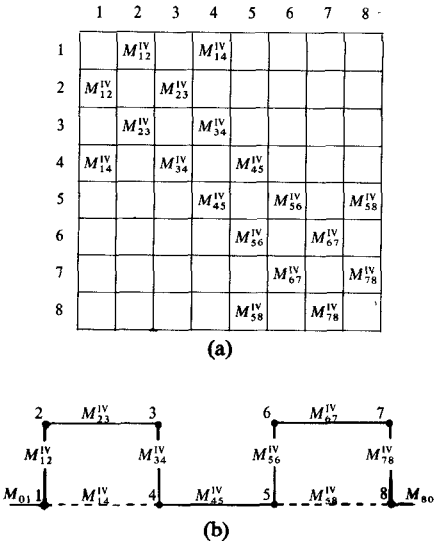

Fig. 6. (a) 8th order CQ coupling matrix. (b) 8th order CQ routing and coupling diagram.

TABLE III
10TH ORDER PRELIMINARY ROTATIONS

Rotation no r	Pivot $[i,j]$	$\theta_r = \tan^{-1}(+M_{u1,u2}/M_{v1,v2})$ $u1$	$u2$	$v1$	$v2$
1	[3, 7]	3	8	7	8
2	[4, 6]	4	7	6	7

It is the quadratic equation for $\tan\theta_1$ in (7) that sets the realizability conditions for this CQ in-line realization. As was mentioned previously these conditions appear to be different from those for the symmetric in-line structure, and it became possible to construct a laboratory model using the CQ procedure possessing both a real-axis and an imaginary axis zero-pair. The measured performance curves of this filter are given below.

B. 10th Order CQ Solution

Fortunately the solution for the 10th order CQ structure uses the same formulas as the 8th order, and a rederivation is not necessary. It is necessary however to first shift the elements of the antidiagonal towards the upper left corner by one (Fig. 7). This is achieved by two preliminary rotations, defined in Table III. Now the formulas (7) may be applied to the upper left 8×8 submatrix, after which a CQ coupling matrix for the 10th order will appear (see Fig. 4).

V. PRACTICAL MODELS

A. 14th Order Linear Phase Filter

The European Communication Satellite (ECS) repeater is a double conversion type, the receiver is at 14 GHz, the IF at about 1 GHz and the power amplifier is at about 11.5 GHz. Demultiplexion of the 6 QPSK 60-MBd uplink channels is achieved at IF by 14th order linear phase filters of interdigital construction. Modern FET technol-

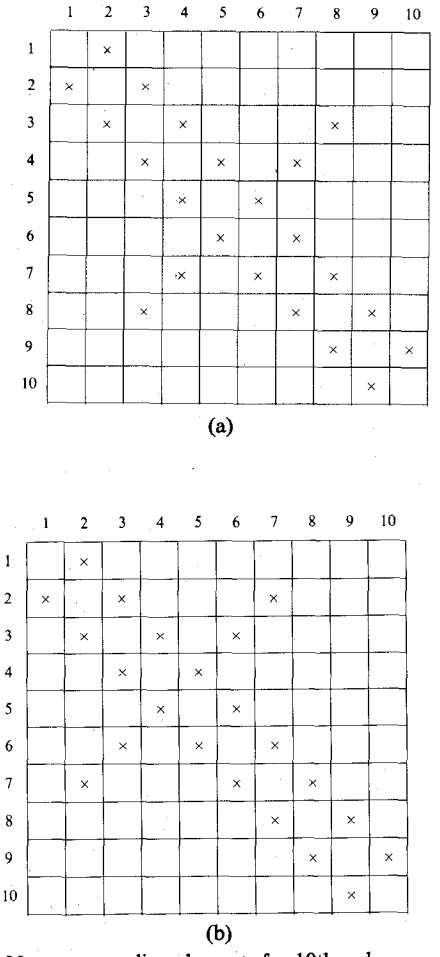

Fig. 7. (a) Nonzero coupling elements for 10th order generalized cross-coupled array. (b) Nonzero coupling elements after the two preliminary rotations.

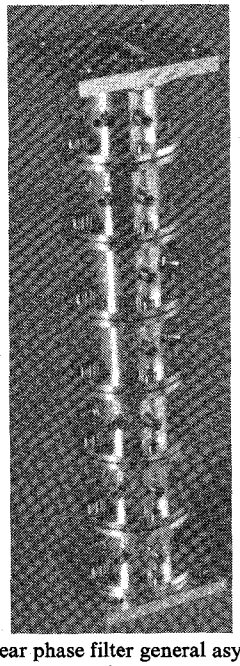

Fig. 8. 14th order linear phase filter general asymmetric in-line realization.

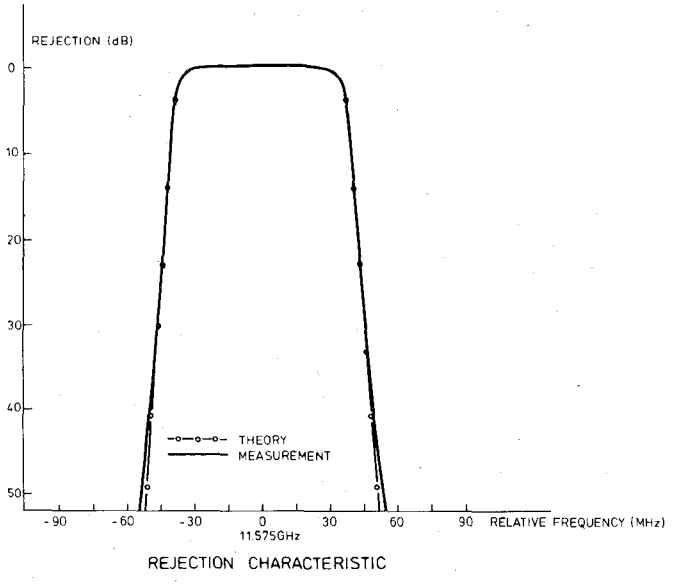

Fig. 9. Rejection characteristic.

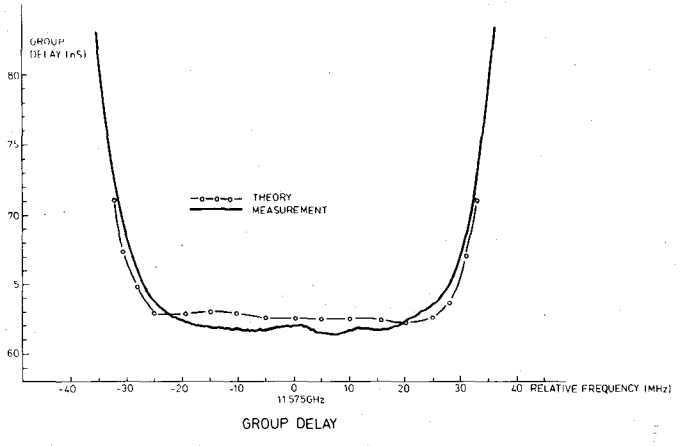

Fig. 10. Group delay response.

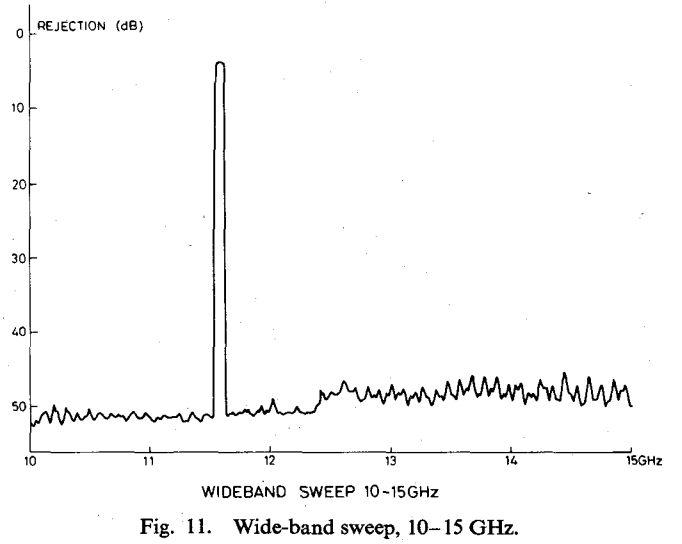

Fig. 11. Wide-band sweep, 10–15 GHz.

TABLE IV
14TH ORDER LINEAR PHASE LOW-PASS PROTOTYPE VALUES

Cross-coupled network prototype element values		General asymmetric realisation prototype coupling values			
$C_1 = C_{14} = 0.9239$	$K'_{1,14} = 0.0$	$M_{12} = 0.8581$	$M_{89} = 0.4064$	$M_{14} = 0.0$	
$C_2 = C_{13} = 1.4698$	$K'_{2,13} = 0.0$	$M_{23} = 0.5961$	$M_{9,10} = 0.4408$	$M_{36} = 0.1090$	
$C_3 = C_{12} = 1.9147$	$K'_{3,12} = 0.0$	$M_{34} = 0.5384$	$M_{10,11} = -0.7332$	$M_{58} = 0.1041$	
$C_4 = C_{11} = 1.7309$	$K'_{4,11} = 0.0397$	$M_{45} = 0.4306$	$M_{11,12} = 0.3029$	$M_{710} = 0.1309$	
$C_5 = C_{10} = 2.0305$	$K'_{5,10} = 0.2257$	$M_{56} = 0.4883$	$M_{12,13} = 0.2460$	$M_{912} = 0.1850$	
$C_6 = C_9 = 1.8850$	$K'_{6,9} = 0.3922$	$M_{67} = -0.6315$	$M_{13,14} = 0.6699$	$M_{11,14} = 0.5363$	
$C_7 = C_8 = 3.2919$	$K'_{7,8} = 0.6111$	$M_{78} = 0.4769$			
All K inverters = 1.0 except K_{78}					

TABLE V
8TH ORDER SELF-EQUALIZED PSEUDOELLIPTIC LOW-PASS PROTOTYPE VALUES

Cross coupled network elements		CQ realised coupling elements			
$C_1 = C_8 = 0.8248$	$K'_{18} = 0.0$	$M_{12} = 0.8904$	$M_{56} = 0.4621$		
$C_2 = C_7 = 1.4310$	$K'_{27} = -0.0854$	$M_{23} = 0.4728$	$M_{67} = 0.8437$		
$C_3 = C_6 = 1.8302$	$K'_{36} = -0.0833$	$M_{34} = 0.5782$	$M_{78} = 0.8368$		
$C_4 = C_5 = 1.7643$	$K_{45} = 1.1344$	$M_{45} = 0.5648$	$M_{14} = 0.2335$		
			$M_{58} = -0.3835$		
$K_{12} = K_{23} = K_{34} = K_{56} = K_{67} = K_{78} = 1.0$					

ogy has made practical the concept of a single conversion repeater with the IF at the downlink frequency of 11.5 GHz and consequent savings in complexity and weight. Thus the demultiplexion function has to be performed at 11.5 GHz instead of 1 GHz and the interdigital technology becomes unsuitable.

To investigate the performance of the single conversion repeater system, a laboratory model has been built and for that a 14th order linear phase dual mode filter constructed using the general asymmetric in-line procedure described above. The prototype is an equiripple amplitude type with group delay equalization over about 75 percent of the design bandwidth of 77 MHz. This is achieved with 6 finite transmission zeros (the maximum permissible, from (1)), arranged in a complex quartet and a real-axis pair. Center frequency is 11 575 MHz, channel 5. The prototype generalized low-pass cross-coupled network element values (see Fig. 1) and prototype asymmetric in-line realized coupling values for this filter are given in Table IV.

Having synthesized the generalized cross-coupled array and then applying the rotations given for the 14th order in Table I, the dual mode filter shown in Fig. 8 was manufactured. The performance is shown in Fig. 9 (amplitude), Fig. 10 (group delay), and Fig. 11 (wide-band sweep to search for spurious responses, particularly in the receive band 14–14.5 GHz). Band center loss is about 3.5 dB corresponding to a Q_u of about 4500, which is somewhat low, but should improve with cavity polishing and plating. Comparing the responses with those for the 1-GHz flight models, the performance seems to be everywhere equivalent except for a slight "rounding of the shoulders" near cutoff, which should be rectified by improving the unloaded Q of the cavities.

B. 8th Order Cascade Quadruplet Filter

Future satellite communication systems are likely to move away from crowded *L*-, *C*-, and *X*-band frequencies to the more spacious 20–30-GHz regions as technology progresses. A breadboard laboratory model has been assembled at ESTEC designed for an uplink frequency of about 30 GHz, a downlink of about 20 GHz, an IF of 11.550 GHz and to carry a single QPSK channel at 30, 60, or 90 MBd [4]. To investigate the degradation introduced by this channel as if it were in a multichannel environment, an 8th order CQ dual mode input multiplexer filter was manufactured using the CQ realization procedures described above, to contiguous PSK channel specifications. The prototype is an equiripple amplitude type with a single imaginary-axis transmission-zero pair to provide an attenuation pole pair, and a real-axis zero pair for group delay equalization over about 60 percent of the filter's 120-MHz bandwidth. Center frequency is 11 550 MHz.

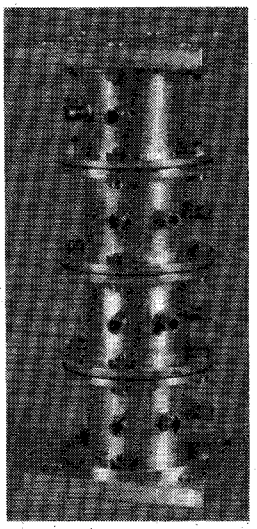

Fig. 12. 8th order self-equalized pseudoelliptic filter, CQ realization.

The initial generalized low-pass cross-coupled network element values (see Fig. 1) and the final CQ realized coupling values for this filter are given in Table V. The laboratory model is shown in Fig. 12 and the performance

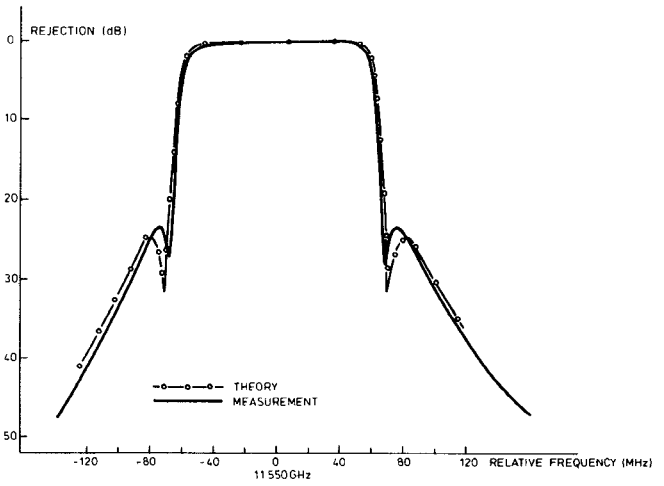

ATTENUATION CHARACTERISTIC

Fig. 13. Attenuation characteristic.

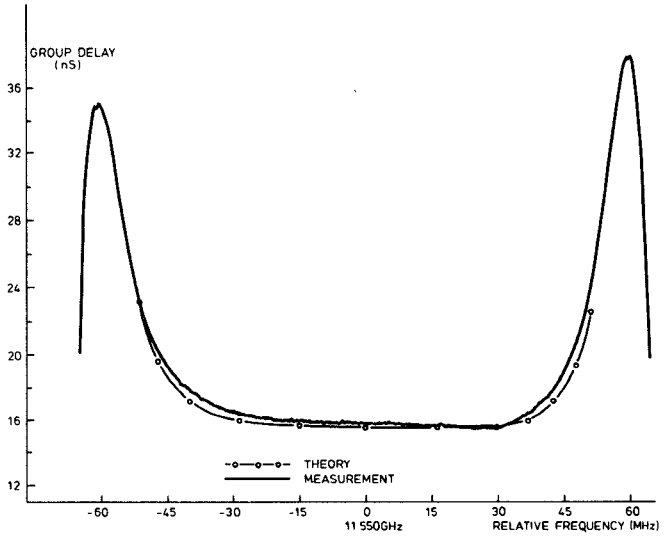

GROUP DELAY CHARACTERISTIC

Fig. 14. Group delay response.

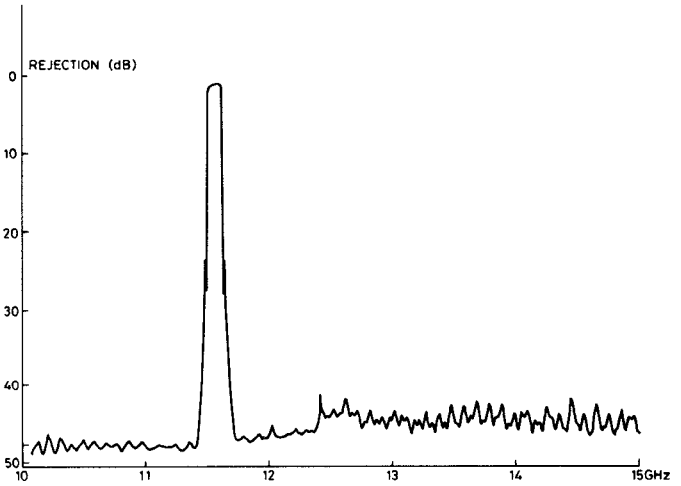

WIDEBAND SWEEP

Fig. 15. Wide-band sweep 10–15 GHz.

is given in Fig. 13 (amplitude), Fig. 14 (group delay), and Fig. 15 (wide-band sweep to search for spurious responses). The BER of the system was measured where it was found that the filter was contributing about 0.2 dB of degradation to the total (see also [5] for a description of a 40-MHz bandwidth version of this filter).

VI. Conclusions

Presented in this paper are two methods for realizing prototype filter characteristics in asymmetric dual mode in-line structures. Together with the symmetric-structure procedure outlined in [2] they provide a comprehensive solution in the area of microwave filter realization. The two procedures are both easily programmed onto a digital computer, and exact answers are produced at the expense of negligible amounts of computer time. Using such programs two dual mode bandpass filters have been constructed, one in the general asymmetric in-line structure and the other in the CQ structure. Their performance curves have been presented to demonstrate their practicality.

References

[1] A. E. Atia and A. E. Williams, "Narrow bandpass waveguide filters," *IEEE Trans. Microwave Theory Tech.*, vol. MTT-20, pp. 258–265, Apr. 1972.

[2] J. D. Rhodes and I. H. Zabalawi, "Synthesis of symmetric dual mode in-line prototype networks," *Int. J. Circuit Theory Appl.*, vol. 8, no. 2, pp. 145–160, Apr. 1980.

[3] J. D. Rhodes, "A low pass prototype network for microwave linear phase filters," *IEEE Microwave Theory Tech.*, vol. MTT-18, pp. 290–300, June 1970.

[4] A. D. Woode, "The characterisation of an experimental laboratory 30/20GHz satellite repeater for digital transmission," in *9th European Microwave Conf. Proc.*, (Brighton, England), Sept. 1979, pp. 223–227.

[5] R. J. Cameron, "Computer aided design of advanced microwave filters," *Proc. SPACECAD '79*, (Bologna, Italy) Sept. 1979, pp. 357–362.